

Total Syntheses of Diketopiperazine Alkaloids via Divergent C3–N1' and C3–C5' Bond Anchor

Bei Fu, Chengliang Li, Leiyang Bai,* and Xuefeng Jiang*

Abstract: Diketopiperazine alkaloids are typically soldered via an inner tryptophan–tryptophan linkage diversely from C3–carbon/nitrogen anchor. The manifold stereochemical frameworks afford broad spectrum of pharmacological activities, meanwhile pose formidable challenges for the efficient synthesis of these alkaloids, particularly in addressing chemoselectivity, regioselectivity, and stereoselectivity. Herein, we disclosed a divergent oxidative coupling between designed **8** and aniline derivatives **13** via the steerable iodine-releasing reagent **14**, achieving the divergent total syntheses of diketopiperazine alkaloids via C3–N1' and C3–C5' bond anchor. The electronic and steric attributes from aniline govern chemo- and site-selectivity for the linkage, enabling programmable assembly for divergently anchored alkaloids libraries. This approach established a stereospecific platform for the unified synthesis of three bioactive alkaloids via a dominant *endo*-selective manifold: (+)-tetratryptomycin B, (+)-pestalazine B, and (+)-*iso*-naseazeine B. The aniline-regulated paradigm unlocked cross-coupling with predictable selectivity for C3-centered alkaloid syntheses.

Introduction

Diketopiperazines, serve as a prototypical pharmacophoric motif with robust protein-binding capacity, functional modulation efficacy, and broad-spectrum biological activities.^[1,2] Dual diketopiperazines were typically anchored on a diversely linked tryptophan–tryptophan core, not only assembling distinct amino acids to strengthen three-dimensional structural complexity, but also bringing multifaceted biological activities (Figure 1A).^[3–7] For example, (+)-tetratryptomycin B^[8] **1** is a tryptophan tetramer linked from C3–N1'; both (+)-WIN 64 821^[9] **2** and (+)-asperazine^[10] **5** are integrated with two tryptophan and two phenylalanine, in which the former is soldered by C3–C3' and

the latter is linked by C3–C7'; (+)-*iso*-naseazeine B^[11] **3** and (+)-naseazeine B^[12] **4** are dimerized via C3–C5' and C3–C6' type for tryptophan–tryptophan core, respectively. The polycyclic diketopiperazine alkaloids dimerized at distinct chemical sites with intensive quaternary carbons arouse huge challenges for controlling the synthetic chemoselectivity, regioselectivity, and stereoselectivity. To achieve the diverse C3–carbon/nitrogen-linked diketopiperazine alkaloids, elegant contributions were reported via a cross-coupling between tryptamine and tryptamine/indoline (C3–N1'^[13] and C3–C3'^[14]) by Kawasaki, via a photoiridium driven enantioselective synthesis (C3–N1'^[15] and C3–C3'^[15]) by Knowles, via an arylative dimerization (C3–N1'^[16] C3–C5',^[11] C3–C6',^[11] and C3–C7'^[17]), a reductive dimerization (C3–C3'^[18–21]), a solvent-caged unsymmetrical diazene fragmentation (C3–C3'^[22–27]), and a final-stage oxidative dimerization (C5–C5'^[28]) by Movassaghi, via an electrophilic amination (C3–N1'^[29–31]) and a silver-mediated alkylation (C3–C5'^[32]) by Baran, via a stereoselective oxidative dimerization^[33] by Jiang (C3–N1'^[34] and C3–C3'^[35]), and others^[36–39] (Figure 1B). The biosynthesis for dimerization linked at C–C bond is attributed to an oxidative radical coupling,^[40] whereas linkage at C–N bond is still not clear.^[5,7] Considerable advances^[3–7,41–48] was achieved for total syntheses of natural products bearing scaffolds **1–5**, the development of generalizable strategies enabling stereochemical diversification for diketopiperazine alkaloids from unified precursors remains a critical unmet demand in contemporary synthetic methodology. Continuous with our efforts on the total syntheses of alkaloids,^[34,35,49–56] tetratryptomycin B **1** (C3–N1') and *iso*-naseazeine B **3** (C3–C5') are anticipated to be achieved via a controllable oxidative coupling between our designed constitutional isomer of tryptophan **8**^[34,35] (Figure 1C). Removal of the diketopiperazine subunits (tryptophan and proline)

[*] B. Fu, C. Li, L. Bai, X. Jiang

Hainan Institute of East China Normal University, State Key Laboratory of Petroleum Molecular & Process Engineering, Shanghai Key Laboratory of Green Chemistry and Chemical Process, School of Chemistry and Molecular Engineering, East China Normal University, 3663 North Zhongshan Road, Shanghai 200062, P. R. China

E-mail: lybai@chem.ecnu.edu.cn
xfjiang@chem.ecnu.edu.cn

X. Jiang

State Key Laboratory of Organometallic Chemistry, Shanghai Institute of Organic Chemistry, Chinese Academy of Sciences, 345 Lingling Road, Shanghai 200032, P. R. China

X. Jiang

State Key Laboratory of Fluorine and Nitrogen Chemistry and Advanced Materials, Shanghai Institute of Organic Chemistry, University of Chinese Academy of Sciences, Chinese Academy of Sciences, 345 Lingling Road, Shanghai 200032, P. R. China

Additional supporting information can be found online in the Supporting Information section

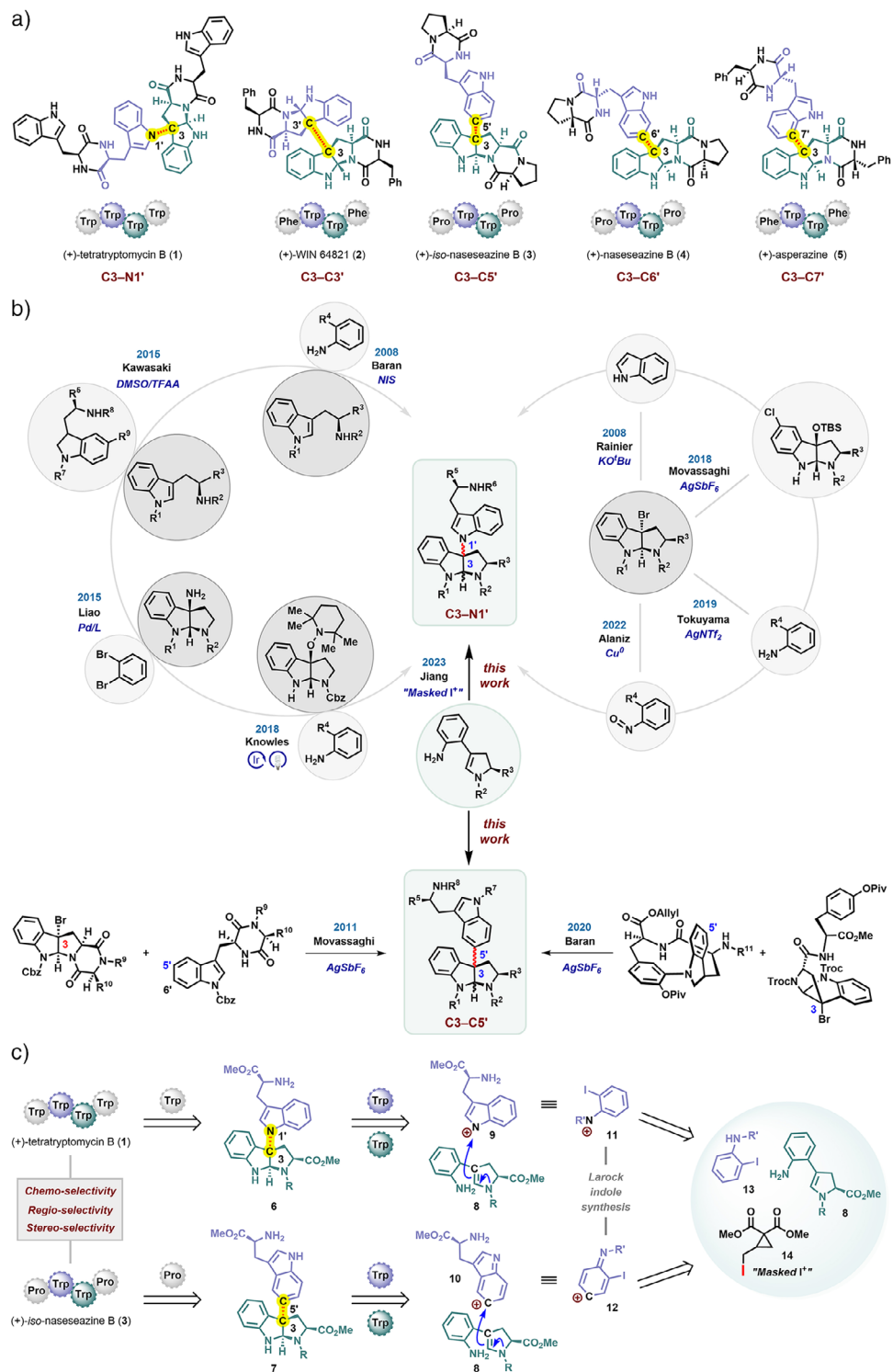


Figure 1. Controllable total syntheses of C3–N1' and C3–C5' linked diketopiperazine alkaloids. A) Representative diketopiperazine alkaloids with diverse linkages. B) Representative tactics for construction of C3–N1' and C3–C5' linkages. C) The tunable aniline-oxidative-coupling for controllable linkage of C3–N1' and C3–C5'.

in **1** and **3** affords a pair of unsymmetrical C3–N1' and C3–C5' connected tryptophan–tryptophan dimer **6** and **7** (highlighted with purple and green in two parts), respectively. The below pyrroloindoline motif of **6/7** deduces the chiral aniline–enamine conjugate **8** via cyclization.

For the upper tryptophan segment of **6/7**, *o*-idoaniline derivatives **13** are employed as its surrogate via a Larock indolization.^[29–31] Therefore, a cationic-based oxidative dimerization via nucleophilic addition from enamine of **8** to tryptophan species **9/10** is equivalent to that

via nucleophilic addition from enamine of **8** to aniline species **11/12**.

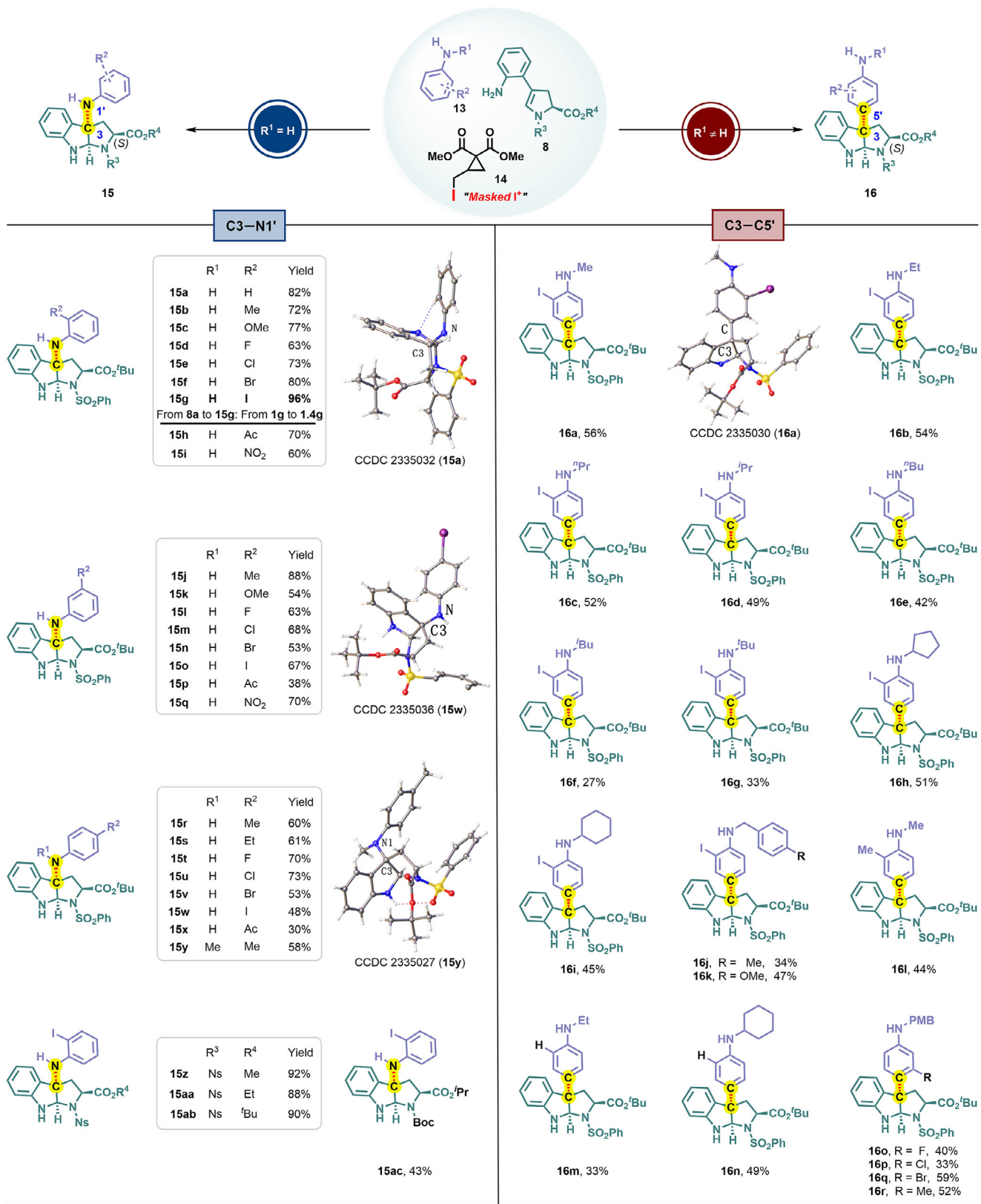
Results and Discussion

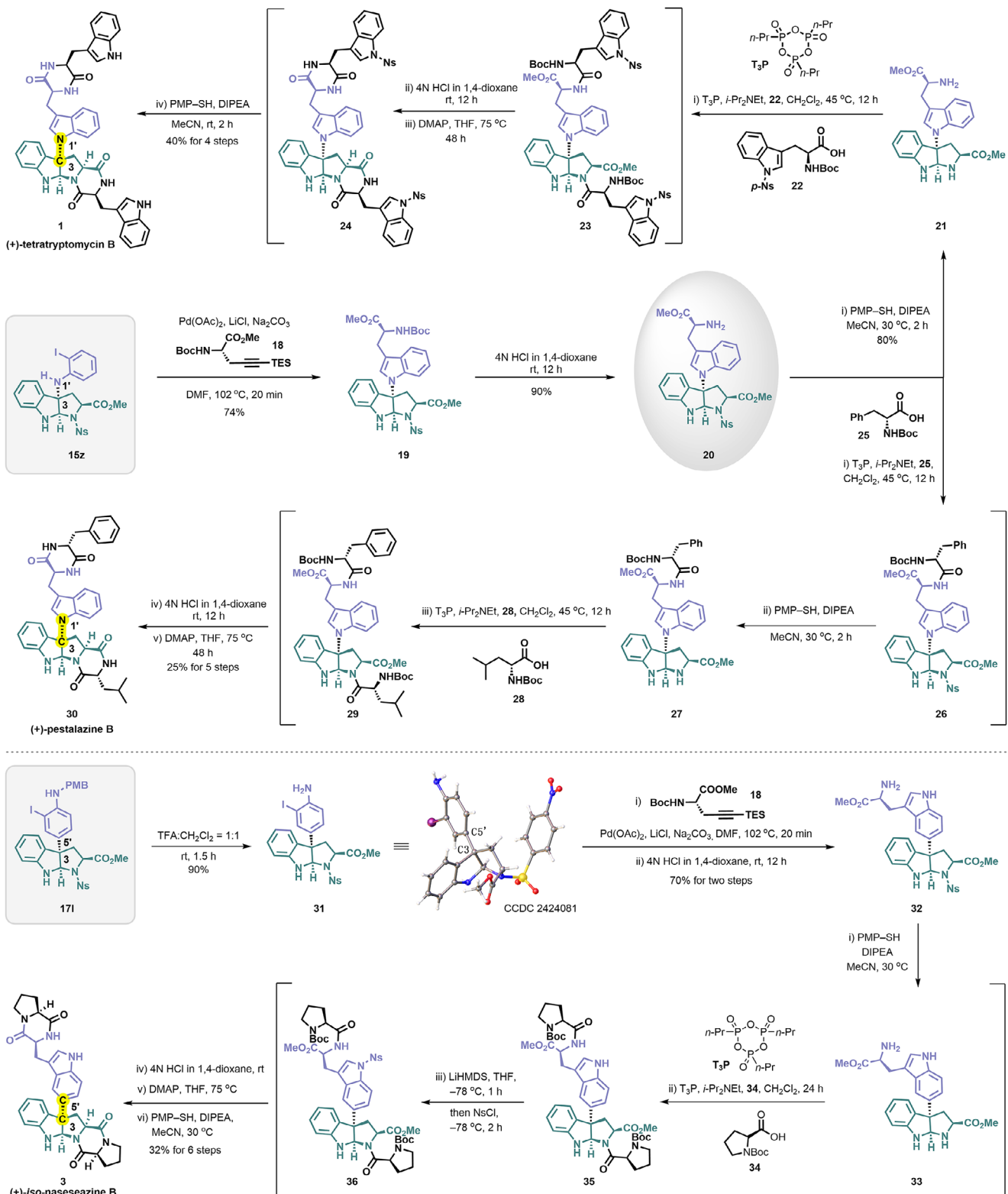
With the optimized conditions in hand (Tables S1–S3), the establishment of C3–N1' linked (+)-tetratryptomycin B **1** and C3–C5' linked (+)-*iso*-naseazaine B **3** scaffold libraries were explored comprehensively (Table 1 and Table 2). It was found that the steric and electronic effects of substituents on amino group from aniline are critical determinants for the coupling selectivity and efficiency, serving as a pivotal handle for divergent construction via C3–N1' and C3–C5' linkages: i) both dual-substituted tertiary aniline (Me and Bn) and mono-substituted electron-withdrawing groups ($R^1 = Ac, Boc, Cbz$, and Ts) cannot afford the coupling products (Table S5), implying the demand for oxidizing site on aniline; ii) unprotected aniline with electron-neutral group and the least steric hindrance ($R^1 = H$) delivered the C3–N1' conjugation (**15a**–**15x** and **15z**–**15ac**, Table 1); iii) the electron-donating groups with sterically enhanced congestion ($R^1 \neq H$) switched to the C3–C5' ligation (**16a**–**16r**, Table 1 and **17a**–**17r**, Table 2). Initially, unprotected aniline adduct **15a** was isolated in 82% yield, whose absolute configuration was further confirmed via X-ray crystallographic analysis, demonstrating an intensive skeleton jointed at C3–N1' between hexahydropyrroloindole and aniline with specific *endo* selectivity. Electron-neutral ($R^2 = H$), electron-donating ($R^2 = Me, Et, OMe$), and electron-withdrawing groups ($R^2 = F, Cl, Br, I, Ac$, and NO_2) at the *ortho*- (**15a**–**15i** and **15z**–**15ac**), *meta*- (**15j**–**15q**), and *para*- (**15r**–**15y**) position of the anilines were well compatible, affording moderate to excellent yields with sole stereoselectivity. X-ray diffraction analysis of **15w** and **15y** further demonstrated the structural accuracy. Notably, *o*-idoaniline hybrid product **15g** was obtained in 91% yield with gram-scaled process. To streamline downstream derivatization of *o*-idoaniline in natural product total synthesis, we systematically evaluated the cross-coupling feasibility with its derivatives (**16a**–**16r**, Table 1 and **17a**–**17r**, Table 2). Following the regulation of site-selectivity, *N*-alkylated aniline substrates (**16a**–**16r**), such as cyclopentyl (**16h**), cyclohexyl (**16i**), and benzyl (**16j** and **16k**) groups, underwent efficient cross-coupling to deliver C3–C5'-linked products with exceptional *endo*-selectivity, further demonstrated by X-ray study of **16a**. Notably, *N*-methyl-*o*-toluidine furnished the anticipated C3–C5' coupling (**16l**), whereas *N*-methyl-*p*-toluidine exclusively afforded the C3–N1' adduct **15y** under identical conditions, further demonstrated via its X-ray analysis (Table 1). This sharp contrast unambiguously demonstrated that *p*-substituents on the aniline core, even with *N*-alkylation, enforce regioselective C–N bond formation, completely suppressing the alternative C–C coupling pathway required for dearomatization, rigorously refined the above empirical rule. The iodo substituent on the aniline exhibited a negligible effect on the reaction efficacy (**16b** versus **16m**; **16i** versus **16n**). Given the pivotal role of **16** as a precursor to the tryptophan unit via the Larock indolization^[29–31] in the total synthesis of (+)-

iso-naseazaine B **3**, we developed an optimized strategy leveraging *p*-nitrobenzenesulfonyl (Ns) building blocks (**8b**, $R^3 = Ns, R^4 = Me$) to enhance scaffold assembly efficiency (**17a**–**17r**, Table 2). Compared to benzenesulfonyl ($PhSO_2$) **8a** ($R^3 = PhSO_2, R^4 = 'Bu$), this electronic modulation not only dramatically improved the C3–C5' ligation yields, but also maintained exceptional stereo-control. Both sterically undemanding linear alkyl groups (**17a**–**17f**) and conformationally restricted cyclic alkyl substituents (**17h**–**17j**) displayed excellent compatibility. Benzyl substituent bearing electron-neutral (**17m**), electron-donating (**17n**–**17p**), and electron-withdrawing (**17q**) functional groups were systematically evaluated, in which the *p*-methoxybenzyl moiety (PMB, **17n**) was the best choice as the optimal protecting group for the natural product synthesis, owing to its highly coupling efficiency (74% yield) and facile removal under mild acidic conditions. It was worth noting that *meta*-substituted anilines (**16o**–**16r** and **17r**) were well tolerated. Accordingly, a 29-membered library of C3–N1' linked tetratryptomycin B **1** scaffold and a 36-membered library of C3–C5' linked *iso*-naseazaine B **3** scaffold have been established with excellent stereo-selectivity efficiently.

Based on the electron-deficient effect and facile removal property of Ns (Table 2), **15z** (Table 1) was synthesized from our protocol for the total synthesis of C3–N1' linked diketopiperazine alkaloid (Scheme 1). The upper tryptophan unit from tryptophan–tryptophan core **19** was achieved in 74% yield via Larock indolization. Strategic removal of the *N*-Boc group under acidic conditions released the free amino product **20** in 90% yield, severing as the common skeleton for divergent synthesis. Treatment with *p*-methyl thiophenol (PMP–SH) and *N*, *N*-diisopropylethylamine resulted in globally deprotected product **21** in 80% yield. T_3P -mediated peptide condensation with tryptophan derivative **22** afforded tetrapeptide **23** without further purification. Two diketopiperazine units (**24**) were constructed via intramolecular ester–amine exchange, followed by sequential deprotection of *N*-Boc groups and alkalization. Dual Ns deprotection under PMP–SH delivered (+)-tetratryptomycin B^[8,57] **1** in 40% yield within 4 steps for the first-time total synthesis. To demonstrate the protocol versatility, structurally diverse diketopiperazine scaffold were installed via a sequential assembly from different amino acids. *N*-Boc-D-phenylalanine **25** was coupled with **20** to obtain tripeptide **26** without further purification. Deprotection of Ns group liberated the reactive amine site, which subsequently underwent T_3P -mediated coupling with *N*-Boc-D-Leu **28** to furnish the tetrapeptide **29**. Subsequent removal of the *N*-Boc groups released free amino under acidic conditions to promote the ester-amine exchange under alkalization, constructing the distinct diketopiperazine motifs, thereby affording (+)-pestalazine B^[16,58–60] **30** in 25% yield within 5 steps. Meanwhile, the total synthesis was launched via **17l** for C3–C5' linked diketopiperazine alkaloid (Scheme 1). Deprotection of PMB protecting group afforded **31** in 90% yield under the presence of trifluoroacetic acid, in which the serried environment of the C3 stereocenter was rechecked via X-ray^[61] study. Subsequent Larock indolization and deprotection of *N*-Boc group delivered the C3–C5' connected tryptophan dimer **32** in 70% yield within 2 steps.

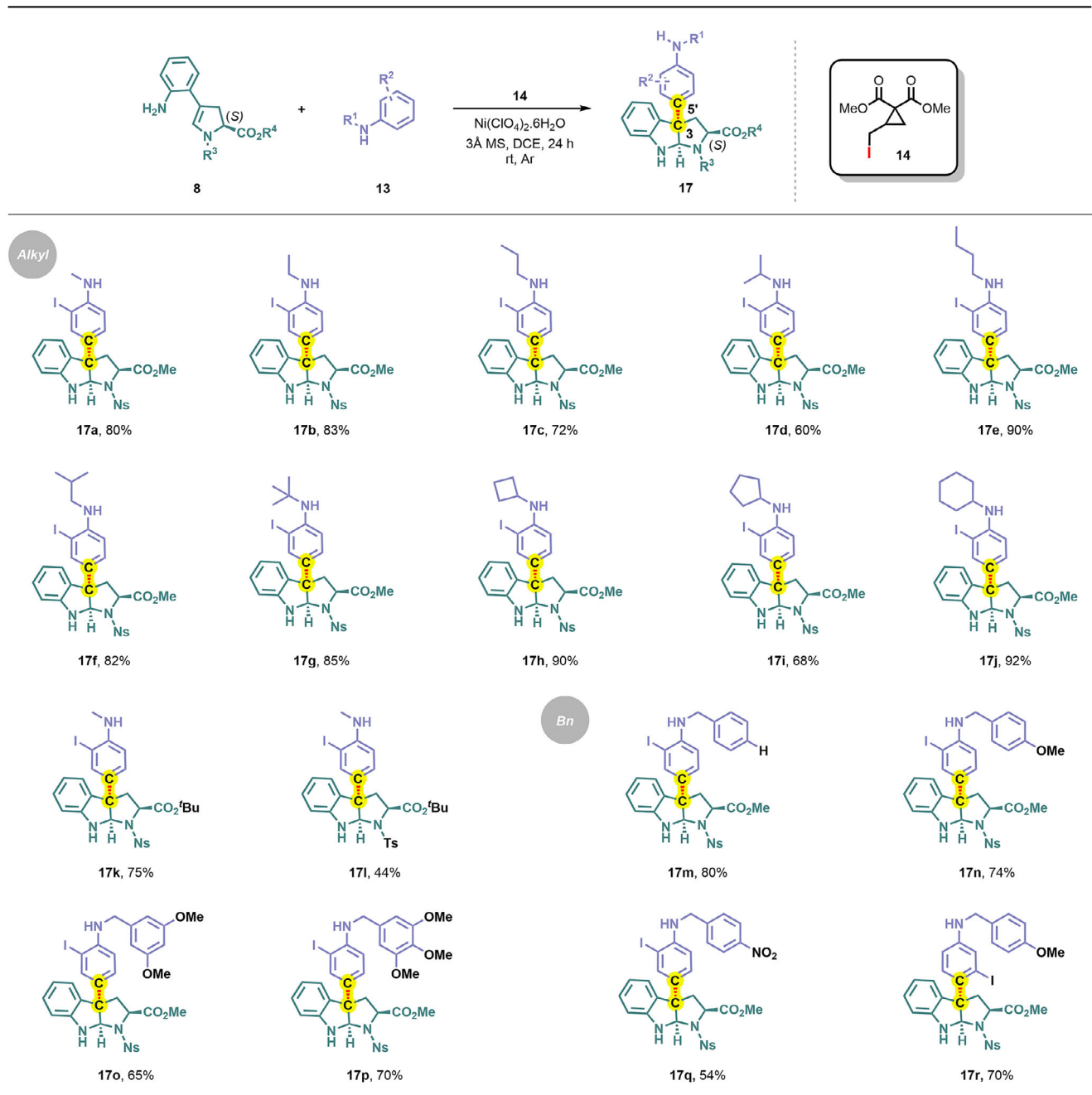
Table 1: Two libraries of C3–N1' linked tetrathyptomyycin B **1** and C3–C5' linked iso-naseseazine B **3** scaffold. ^{a)} Reaction conditions: **8** (0.5 mmol), **13** (5 equiv.), **14** (1.1 equiv.), $\text{Ni}(\text{ClO}_4)_2 \cdot 6\text{H}_2\text{O}$ (10 mol%), 1,2-Dichloroethane (DCE, $c = 0.01$), 3 Å MS, rt, argon, 24 h, isolated yields.





Scheme 1. Total syntheses of tetrathyptomyycin B (**1**), (+)-pestalazine B (**30**), and (+)-*iso*-naseazeaine B (**3**).

Table 2: C3–C5' linked iso-naseseazine B **3** scaffold library. ^{a)}Reaction conditions: **8** (0.5 mmol), **13** (5 equiv.), **14** (1.1 equiv.), Ni(ClO₄)₂·6H₂O (10 mol%), DCE ($c = 0.01$), 3 Å MS, rt, argon, 24 h, isolated yields.



Following the similar sequences of Ns groups ejection, dual peptide condensation, cyclization via ester–amine exchange, (+)-iso-naseseazine B^[11] **3** was obtained in 32% yield for 6 steps, in which the diketopiperazine scaffold was established via *N*-Boc-L-Proline **34**. It is noteworthy that the exposed amino group of tryptophan (**35**) should be shielded by Ns group to avoid the acid-mediated decomposition. The divergent synthesis of these three natural products demonstrated the great potential for modular installation via versatile amino acid building blocks towards both linear and angular diketopiperazine alkaloids (Scheme 1).

To elucidate the mechanism of regioselectivity and stereoselectivity in the aniline-controlled oxidative coupling, density functional theory (DFT) calculations and visualization of weak interactions were conducted (Figure 2). The aniline and **8b** were strategically employed to demonstrate site-selective C3–N1' bond formation, achieving favorable *endo*-configuration, corroborated by crystallographic analysis (Figure 2A). Transition state analysis revealed that the C–C coupled product (**Ts-1-C-C-endo**) was energetically disfavored by 1.5 kcal/mol compared to its C–N counterpart (**Ts-1-C-N-endo**), explaining the observed C–N selectivity. The

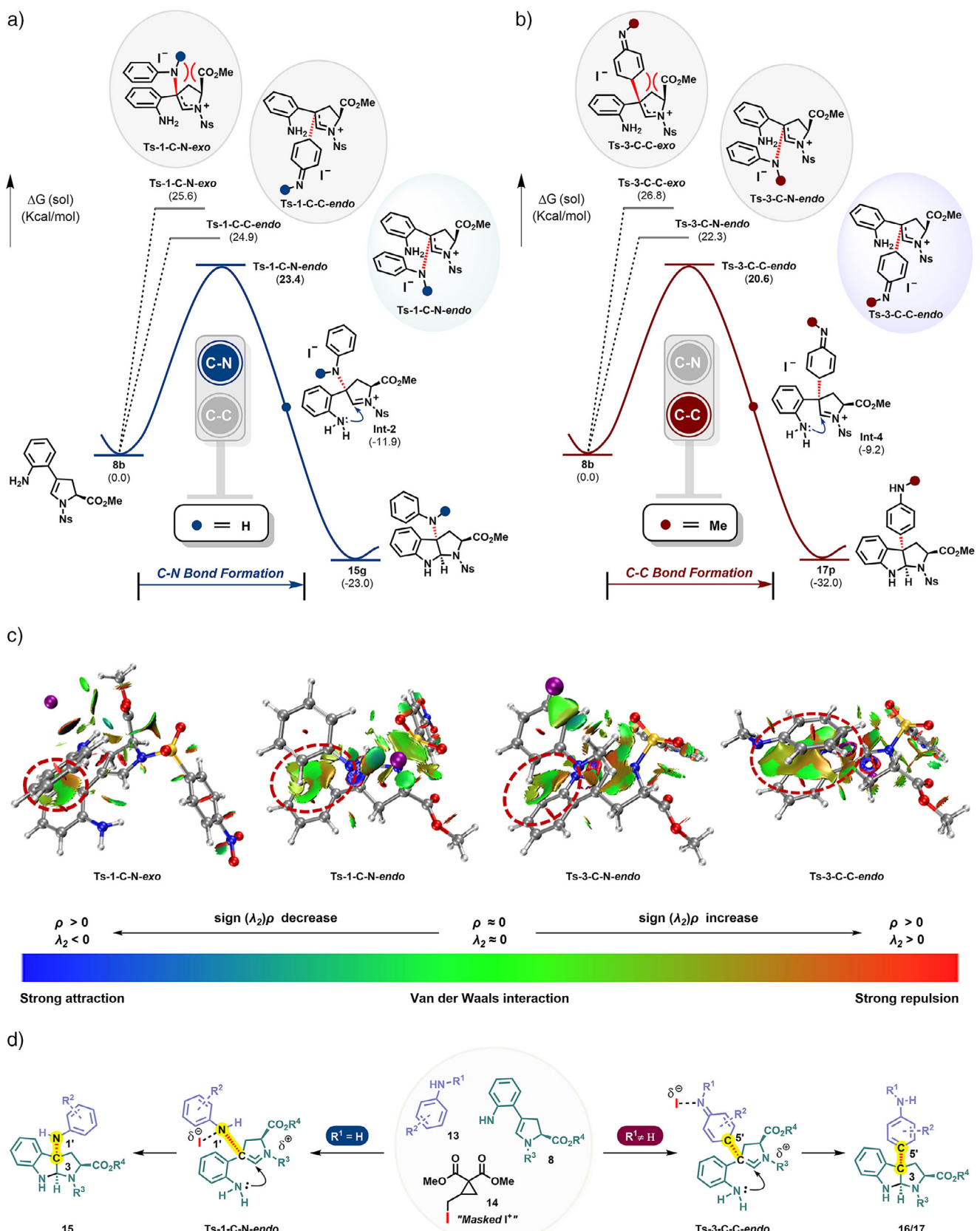


Figure 2. Computational investigations of regioselectivity and stereo-selectivity. A) Free energy profile for the coupling of aniline and **8b** (Gibbs free energies are given in kcal/mol). B) Free energy profile for the coupling of *N*-methyl-aniline and **8b** (Gibbs free energies are given in kcal/mol). C) Visualization of weak interactions by Multiwfn.^[62,63] D) Proposed mechanism for the tunable-aniline-oxidative coupling.

exo stereoisomer (**Ts-1-C-N-exo**) exhibited a 2.2 kcal/mol higher energy barrier relative to the *endo* configuration (**Ts-1-C-N-endo**). Pronounced $\pi-\pi$ interactions between the benzene of aniline and **8b** (highlighted in green and marked with red circles in two parts) preferentially stabilized *endo* pathway (**Ts-1-C-N-endo**) through effective dispersion force (Figure 2C). On the other hand, *N*-methylaniline and **8b** were selected to investigate regioselective C–C bond formation and *endo*-configuration stereocontrol (Figure 2B). Computational analysis demonstrated a complete reversal in regioselectivity, favored by 1.7 kcal/mol with the C–C-addition pathway (**Ts-3-C-C-endo**) compared to the competing C–N pathway (**Ts-3-C-N-endo**). This regioselective preference for C–C bond formation was attributed to significant $\pi-\pi$ interactions between the aminoquinone from aniline and **8b**, which effectively stabilized the transition state **Ts-3-C-C-endo** (Figure 2C). Additionally, the *exo* stereo-isomer (**Ts-1-C-C-exo**) was determined to be energetically unfavorable by 6.2 kcal/mol compared to the *endo* configuration (**Ts-1-C-C-endo**), consistent with the observed experimental stereochemical bias. Based on these, the reaction mechanism was addressed as follow (Figure 2D). First, a catalytic Ni(II) species was preferentially bound to 1,3-dicarbonyl of dicarboxylate **14**, triggering the sustained-release iodine cation (I^+) as the oxidant. When $R^1 = H$, I^+ induced polarity inversion at the aniline nitrogen via an oxidation process. The electrophilic nitrogen center was captured by the enamine of **8** from the backside of the chiral group (*endo* configuration, **Ts-1-C – N-endo**) forming the C3–N1' bond. The iminium cation obtained from enamine isomerization was immediately captured by the amino group from aniline, resulting in the intramolecular cyclization towards the C–N linked adduct **15**. When $R^1 \neq H$ and the *para*-unsubstituted aniline are applied, the nitrogen-centered cationic charge preferentially delocalized to the *para*-position via resonance stabilization, generating a carbocation aminoquinone intermediate. This carbocation was trapped by enamine of **8** in an *endo* stereochemical mode to form the C3–C5' bond, followed by annulation to afford the C–C coupling pathway (**16/17**).

Conclusion

In summary, an oxidative coupling strategy was developed to achieve customizable chemoselectivity, regioselectivity, and stereocontrol for diverse C3-connected dикетопиperазине alkaloid syntheses. By tuning the electronic and steric profiles of aniline derivatives, the protocol enabled divergent access to C3–N1' and C3–C5' linkage via a masked iodine-mediated cationic coupling pathway. Key to this approach was the stereochemical preorganization from enamine–aniline conjugate, directing *endo*-selective conformation. The aniline-regulated oxidative coupling model enabled programmable cross-linkage with predictable selectivity, establishing a platform for assembly of structurally divergent alkaloid families, as exemplified by the unified synthesis of (+)-tetrathyptromycin B, (+)-pestalazine B, and (+)-*iso*-naseazaine B.

Acknowledgements

The authors are grateful for financial support provided by the NSFC (22125103 and 22401095), Shanghai Rising-Star Program (24QB2704700), the STCSM (22JC1401000), and the China Postdoctoral Science Foundation (BX20230127).

Conflict of Interests

The authors declare no conflict of interest.

Data Availability Statement

The data that support the findings of this study are available in the Supporting Information of this article.

Keywords: Aniline-regulated oxidative coupling • C3–C5' linker • C3–N1' linker • Dикетопиperазине alkaloids • *Endo*-selectivity

- [1] A. D. Borthwick, *Chem. Rev.* **2012**, *112*, 3641–3716, <https://doi.org/10.1021/cr200398y>.
- [2] Z. Song, Y. Hou, Q. Yang, X. Li, S. Wu, *Mar. Drugs* **2021**, *19*, 403, <https://doi.org/10.3390/MD19080403>.
- [3] J. Kim, M. Movassaghi, *Acc. Chem. Res.* **2015**, *48*, 1159–1171, <https://doi.org/10.1021/ar500454v>.
- [4] N. G. M. Gomes, R. B. Pereira, *Mar. Drugs* **2019**, *17*, 551, <https://doi.org/10.3390/MD17100551>.
- [5] N. Wang, P. Saidhareddy, X. Jiang, *Nat. Prod. Rep.* **2020**, *37*, 246–275, <https://doi.org/10.1039/C8NP00093J>.
- [6] P. García-Domínguez, A. Areal, R. Alvarez, A. De Lera, *Nat. Prod. Rep.* **2022**, *39*, 1172–1225, <https://doi.org/10.1039/D2NP0006G>.
- [7] C. Sun, W. Tian, Z. Lin, X. Qu, *Nat. Prod. Rep.* **2022**, *39*, 1721–1765, <https://doi.org/10.1039/D2NP00030J>.
- [8] J. Liu, X. Xie, S.-M. Li, *Chem. Commun.* **2020**, *56*, 11042–11045, <https://doi.org/10.1039/D0CC04772D>.
- [9] C. J. Barrow, D. M. Sedlock, *J. Nat. Prod.* **1994**, *57*, 1239–1244, <https://doi.org/10.1021/np50111a008>.
- [10] M. Varoglu, T. H. Corbett, F. A. Valeriote, P. Crews, *J. Org. Chem.* **1997**, *62*, 7078–7079, <https://doi.org/10.1021/jo970568z>.
- [11] J. Kim, M. Movassaghi, *J. Am. Chem. Soc.* **2011**, *133*, 14940–14943, <https://doi.org/10.1021/ja206743v>.
- [12] R. Raju, A. M. Piggott, M. Conte, W. G. L. Aalbersberg, K. Feussner, R. J. Capon, *Org. Lett.* **2009**, *11*, 17, 3862–3865, <https://doi.org/10.1021/ol901466r>.
- [13] M. Tayu, T. Ishizaki, K. Higuchi, T. Kawasaki, *Org. Biomol. Chem.* **2015**, *13*, 3863–3865, <https://doi.org/10.1039/C5OB00190K>.
- [14] M. Tayu, K. Higuchi, T. Ishizaki, T. Kawasaki, *Org. Lett.* **2014**, *16*, 3613–3615, <https://doi.org/10.1021/ol5012373>.
- [15] E. C. Gentry, L. J. Rono, M. E. Hale, R. Matsuura, R. R. Knowles, *J. Am. Chem. Soc.* **2018**, *140*, 3394–3402, <https://doi.org/10.1021/jacs.7b13616>.
- [16] B. M. Nelson, R. P. Loach, S. Schiesser, M. Movassaghi, *Org. Biomol. Chem.* **2018**, *16*, 202–207, <https://doi.org/10.1039/C7OB02985C>.
- [17] R. P. Loach, O. S. Fenton, M. Movassaghi, *J. Am. Chem. Soc.* **2016**, *138*, 1057–1064, <https://doi.org/10.1021/jacs.5b12392>.

[18] M. Movassaghi, M. A. Schmidt, *Angew. Chem. Int. Ed.* **2007**, *46*, 3725–3728, <https://doi.org/10.1002/anie.200700705>.

[19] M. Movassaghi, M. A. Schmidt, J. A. Ashenhurst, *Angew. Chem. Int. Ed.* **2008**, *47*, 1485–1487, <https://doi.org/10.1002/anie.200704960>.

[20] J. Kim, J. A. Ashenhurst, M. Movassaghi, *Science* **2009**, *324*, 238–241, <https://doi.org/10.1126/science.1170777>.

[21] J. Kim, M. Movassaghi, *J. Am. Chem. Soc.* **2010**, *132*, 14376–14378, <https://doi.org/10.1021/ja106869s>.

[22] M. Movassaghi, O. K. Ahmad, S. P. Lathrop, *J. Am. Chem. Soc.* **2011**, *133*, 13002–13005, <https://doi.org/10.1021/ja2057852>.

[23] S. P. Lathrop, M. Movassaghi, *Chem. Sci.* **2014**, *5*, 333–340, <https://doi.org/10.1039/C3SC52451E>.

[24] S. P. Lathrop, M. Pompeo, W.-T. T. Chang, M. Movassaghi, *J. Am. Chem. Soc.* **2016**, *138*, 7763–7769, <https://doi.org/10.1021/jacs.6b04072>.

[25] P. Lindovska, M. Movassaghi, *J. Am. Chem. Soc.* **2017**, *139*, 17590–17596, <https://doi.org/10.1021/jacs.7b09929>.

[26] M. M. Pompeo, J. H. Cheah, M. Movassaghi, *J. Am. Chem. Soc.* **2019**, *141*, 14411–14420, <https://doi.org/10.1021/jacs.9b07397>.

[27] T. Z. Scott, M. Movassaghi, *J. Am. Chem. Soc.* **2024**, *146*, 23574–23581, <https://doi.org/10.1021/jacs.4c07705>.

[28] K. A. D'Angelo, C. K. Schissel, B. L. Pentelute, M. Movassaghi, *Science* **2022**, *375*, 894–899, <https://doi.org/10.1126/science.abm6509>.

[29] T. Newhouse, P. S. Baran, *J. Am. Chem. Soc.* **2008**, *130*, 10886–10887, <https://doi.org/10.1021/ja8042307>.

[30] T. Newhouse, C. A. Lewis, P. S. Baran, *J. Am. Chem. Soc.* **2009**, *131*, 6360–6361, <https://doi.org/10.1021/ja901573x>.

[31] T. Newhouse, C. A. Lewis, K. J. Eastman, P. S. Baran, *J. Am. Chem. Soc.* **2010**, *132*, 7119–7137, <https://doi.org/10.1021/ja1009458>.

[32] S. H. Reisberg, Y. Gao, A. S. Walker, E. J. N. Helfrich, J. Clardy, P. S. Baran, *Science* **2020**, *367*, 458–463, <https://doi.org/10.1126/science.ayy9981>.

[33] L. Bai, X. Jiang, *Chem Catal* **2023**, *3*, 100752–100760.

[34] L. Bai, J. Li, X. Jiang, *Chem* **2023**, *9*, 483–496, <https://doi.org/10.1016/j.chempr.2022.10.021>.

[35] L. Bai, Y. Ma, X. Jiang, *J. Am. Chem. Soc.* **2021**, *143*, 20609–20615, <https://doi.org/10.1021/jacs.1c10498>.

[36] V. R. Espejo, J. D. Rainier, *J. Am. Chem. Soc.* **2008**, *130*, 12894–12895, <https://doi.org/10.1021/ja8061908>.

[37] Q. Li, T. Xia, L. Yao, H. Deng, X. Liao, *Chem. Sci.* **2015**, *6*, 3599–3605;

[38] H. Hakamata, H. Ueda, H. Tokuyama, *Org. Lett.* **2019**, *21*, 4205–4209, <https://doi.org/10.1021/acs.orglett.9b01399>.

[39] J. B. Shaum, A. Nikolaev, H. C. Steffens, L. Gonzalez, S. Walker, A. V. Samoshin, G. Hammersley, E. H. La, J. R. de Alaniz, *J. Org. Chem.* **2022**, *87*, 9907–9914, <https://doi.org/10.1021/acs.joc.2c00923>.

[40] G. W. Kirby, S. W. Shah, E. J. Herbert, *J. Chem. Soc. C* **1969**, 1916, <https://doi.org/10.1039/j39690001916>.

[41] J. A. May, B. Stoltz, *Tetrahedron* **2006**, *62*, 5262–5271, <https://doi.org/10.1016/j.tet.2006.01.105>.

[42] A. Steven, L. E. Overman, *Angew. Chem. Int. Ed.* **2007**, *46*, 5488–5508, <https://doi.org/10.1002/anie.200700612>.

[43] M. A. Schmidt, M. Movassaghi, *Synlett* **2008**, 313–324;

[44] B. M. Trost, M. Osipov, *Chem. - Eur. J.* **2015**, *21*, 16318–16343, <https://doi.org/10.1002/chem.201501735>.

[45] J.-B. Xu, K.-J. Cheng, *Molecules* **2015**, *20*, 6715–6738, <https://doi.org/10.3390/molecules20046715>.

[46] X. Shen, Y. Zhou, Y. Xi, J. Zhao, H. Zhang, *Nat. Prod. Bioprospect.* **2016**, *6*, 117–139, <https://doi.org/10.1007/s13659-016-0092-8>.

[47] X. Shen, T. Peng, Y. Zhou, Y. Xi, J. Zhao, X. Yang, H. Zhang, *Chin. J. Org. Chem.* **2019**, *39*, 2685, <https://doi.org/10.6023/cjoc201903058>.

[48] J. J. Dotson, L. Liepuoniute, J. Logan Bachman, V. M. Hipwell, S. I. Khan, K. N. Houk, N. K. Garg, M. A. Garcia-Garibay, *J. Am. Chem. Soc.* **2021**, *143*, 4043–4054, <https://doi.org/10.1021/jacs.1c01100>.

[49] M. Feng, X. Jiang, *Chem. Commun.* **2014**, *50*, 9690–9692, <https://doi.org/10.1039/C4CC04148H>.

[50] M. Feng, B. Tang, N. Wang, H. Xu, X. Jiang, *Angew. Chem. Int. Ed.* **2015**, *54*, 14960–14964, <https://doi.org/10.1002/anie.201508340>.

[51] D. Ding, T. Mou, M. Feng, X. Jiang, *J. Am. Chem. Soc.* **2016**, *138*, 5218–5221, <https://doi.org/10.1021/jacs.6b01707>.

[52] N. Wang, S. Du, D. Li, X. Jiang, *Org. Lett.* **2017**, *19*, 3167–3170, <https://doi.org/10.1021/acs.orglett.7b01292>.

[53] N. Wang, J. Liu, C. Wang, L. Bai, X. Jiang, *Org. Lett.* **2018**, *20*, 292–295, <https://doi.org/10.1021/acs.orglett.7b03694>.

[54] D. Ding, G. Zhu, X. Jiang, *Angew. Chem. Int. Ed.* **2018**, *57*, 9028–9032, <https://doi.org/10.1002/anie.201804788>.

[55] G. Zhu, W.-C. Gao, X. Jiang, *J. Am. Chem. Soc.* **2021**, *143*, 1334–1340, <https://doi.org/10.1021/jacs.0c13012>.

[56] D. Li, J. Meng, X. Jiang, *CCS Chem.* **2023**, *5*, 2152–2158.

[57] J. J. L. Malit, W. Liu, A. Cheng, S. Saha, L.-L. Liu, P.-Y. Qian, *Org. Lett.* **2021**, *23*, 6601–6605, <https://doi.org/10.1021/acs.orglett.9b01399>.

[58] C. Pérez-Balado, Á. R. D. Lera, *Org. Biomol. Chem.* **2010**, *8*, 5179, <https://doi.org/10.1039/c0ob00531b>.

[59] Q. Li, T. Xia, L. Yao, H. Deng, X. Liao, *Chem. Sci.* **2015**, *6*, 3599–3605, <https://doi.org/10.1039/C5SC00338E>.

[60] H. Hakamata, H. Ueda, H. Tokuyama, *Org. Lett.* **2019**, *21*, 4205–4209, <https://doi.org/10.1021/acs.orglett.9b01399>.

[61] Deposition numbers CCDC **2335032** (**15a**), 2335036 (**15 w**), 2335034 (**15x**), 2335027 (**15y**), 2335030 (**16a**), and 2424081 (**31**) contain the supplementary crystallographic data for this paper. These data are provided free of charge by the joint Cambridge Crystallographic Data Centre and Fachinformationszentrum Karlsruhe [Access Structures service](https://www.ccdc.cam.ac.uk/AccessStructures).

[62] T. Lu, F. Chen, *J. Comput. Chem.* **2012**, *33*, 580–592, <https://doi.org/10.1002/jcc.22885>.

[63] T. Lu, *J. Chem. Phys.* **2024**, *161*, 082503.

Manuscript received: October 02, 2025

Revised manuscript received: November 24, 2025

Manuscript accepted: November 25, 2025

Version of record online: ■■■